


**RESEARCH ARTICLE**

# Global population-weighted degree-day projections for a combination of climate and socio-economic scenarios

Jonathan Spinoni<sup>1</sup>  | Paulo Barbosa<sup>1</sup> | Hans-Martin Füssel<sup>2</sup> |  
Niall McCormick<sup>1</sup> | Jürgen V. Vogt<sup>1</sup> | Alessandro Dosio<sup>1</sup>

<sup>1</sup>European Commission, Joint Research Centre (JRC), Ispra, Italy

<sup>2</sup>Climate Change Impacts, Vulnerability and Adaptation, European Environment Agency (EEA), Copenhagen, Denmark

**Correspondence**

Jonathan Spinoni, European Commission, Joint Research Centre (JRC), Ispra, Italy.  
Email: jonathan.spinoni@ec.europa.eu

**Abstract**

The projected global temperature increase in the 21st century is expected to have consequences on energy consumption due to increase (decrease) in energy demand to cool (heat) the built environments. Such increase (decrease) also depends on the number of end users for such energy, thus it is crucial to include population into the analyses. This study presents population-weighted (w) cooling (CDD), heating (HDD), and energy (EDD) degree-day projections at global, regional, and local scales for the 21st century. We used a large ensemble of high-resolution (0.44°) climate simulations from the COordinated Regional-climate Downscaling EXperiment (CORDEX) to compute degree-days for baseline (1981–2010) and global warming levels (GWLs from 1.5°C to 4°C), based on two representative concentration pathways. We used population projections from the NASA-SEDAC datasets, driven by five socio-economic scenarios (SSPs). The progressive increase in CDD outbalances the decrease in HDD in Central and South America, Africa, and Oceania and the opposite situation is likely to occur in North America, Europe, and Asia; at global scale, they are balanced. However, if results are weighted according to population, the increase in wCDD outbalances the decrease in wHDD almost everywhere for most GWLs and SSPs. Few regions show a decreasing tendency in wEDD at high GWLs for all SSPs: central Europe, northwestern, northeastern, and eastern Asia. Globally, wEDD are likely to double at 2°C compared to 1981–2010 independently of the SSP. Under the worst-case scenario (SSP3), at 4°C wCDD are approximately 380% higher and wHDD approximately 30% lower than in the recent past, leading to an increase in wEDD close to 300%.

**KEYWORDS**

climate projections, CORDEX, degree days, global warming, population, SSPs

This is an open access article under the terms of the Creative Commons Attribution-NonCommercial-NoDerivs License, which permits use and distribution in any medium, provided the original work is properly cited, the use is non-commercial and no modifications or adaptations are made.

© 2021 The Authors. *International Journal of Climatology* published by John Wiley & Sons Ltd on behalf of Royal Meteorological Society.

## 1 | INTRODUCTION

Global warming, which refers to progressive temperature increase observed in the last decades (Field *et al.*, 2014) and projected over the 21st century (Rogelj *et al.*, 2012; IPCC, 2018), has two immediate consequences: higher temperatures would result in an increase (decrease) in energy demand to cool (heat), where required, the indoor environments. However, the science of energy consumption of buildings is complex (Pérez-Lombard *et al.*, 2008; Zhao and Magoulès, 2012), in particular regarding the estimation of thermal comfort (de Dear *et al.*, 2013; Taleghani *et al.*, 2013; Yang *et al.*, 2014), either for residential buildings (Peeters *et al.*, 2009; Manzano-Agugliaro *et al.*, 2015) and non-residential buildings (Wagner *et al.*, 2007; Dounis and Caraiscos, 2009).

Climatology and science related to energy consumption of buildings together aim at estimating the impact of climate change on indoor thermal comfort (Santamouris *et al.*, 2001; Auffhammer and Mansur, 2014). Great attention is dedicated to residential electricity demand in a warming climate (Sailor and Pavlova, 2003; Sathaye *et al.*, 2013; Auffhammer *et al.*, 2017), potentially subjected to unsustainable peaks during heat waves (Dirks *et al.*, 2015), but fundamental to help limiting health issues (Le Tertre *et al.*, 2006).

Despite the difficulties in quantitatively correlating climate and energy consumption of buildings (Huang and Gurney, 2016), a common practice is to estimate the energy required to cool and heat the environment by means of temperature-based indicators, that is, cooling degree-days and heating degree-days (CDD and HDD; Spinoni *et al.*, 2015; Damm *et al.*, 2017). HDD and CDD can be combined into energy degree-days (EDD; Petri and Caldeira, 2015) to estimate the effect of simultaneous increase and/or decrease on energy demand. A limitation of EDD is that they treat changes in HDD and CDD equally, though heating and cooling systems are often based on different technologies, with higher primary energy needs and economic costs for cooling than for heating (Auffhammer and Mansur, 2014; Buceti, 2015).

These indicators, based on temperature thresholds calibrated on indoor thermal comfort (Kendon *et al.*, 2016), are frequently applied to observed meteorological data at country scale, for example, over United States (Alola *et al.*, 2019), Italy (De Rosa *et al.*, 2015), Greece (Papakostas and Kyriakis (2005), Morocco (Idchabani *et al.*, 2015), China (Jiang *et al.*, 2009), South Korea (Lee *et al.*, 2014), Australia (Ahmed *et al.*, 2012), and so on. Similarly, studies on projections of CDD and HDD are available mostly at country and macro-regional scales, for example, for Switzerland (Christenson *et al.*, 2006), Europe (Spinoni *et*

*al.*, 2018), China (Shi *et al.*, 2018), United States (Petri and Caldeira, 2015), and so on.

The computation of degree-days, both for past periods and future projections is not free from uncertainties (Moore *et al.*, 2012; You *et al.*, 2014), due to multiple possible calibration approaches (Holmes *et al.*, 2017), thresholds (Day and Karayiannis, 1999), and assumptions for energy demand of buildings (Day *et al.*, 2000). Being aware of these limitations, the first goal of this study is to improve the state of art of degree-days projections. Following the approach used by Spinoni *et al.* (2018) for Europe, we used simulations from the COordinated Regional-climate Downscaling EXperiment (CORDEX; see: <https://cordex.org/>) to obtain projections of CDD, HDD, and EDD based on different representative concentration pathways (RCPs) in the 21st century. To our knowledge—at the time of writing—this is the first study analysing high-resolution (0.44°) global projections of degree-days based on a large ensemble of regional climate models (RCMs) driven by global climate models (GCMs).

Only very few studies include population in analyses regarding past degree-days at global scale (Atalla *et al.*, 2018), and those at country scale (e.g., for the United States: Guttman, 1983; Canada: Taylor, 1981; Spain: Valor *et al.*, 2001; Italy: Fantini and Schenone, 2001) are rather outdated. No population-weighted (w) wCDD and wHDD global projections are known to us, but focusing only at continental (e.g., for Europe: Spinoni *et al.*, 2018) or country scales, like China (Shi *et al.*, 2018) or the United States (Zhou *et al.*, 2013). Consequently, as second goal of this study, we computed global population-weighted degree-day projections using high-resolution population data (from National Aeronautics Space Administration's Socio-economic Data and Applications Center NASA-SEDAC; Jones and O'Neill, 2016) for five shared socio-economic pathways (SSPs; O'Neill *et al.*, 2014), namely: SSP1 ('green growth'; van Vuuren *et al.*, 2017b), SSP2 ('middle of the road'; Fricko *et al.*, 2017), SSP3 ('regional rivalry'; Fujimori *et al.*, 2017), SSP4 ('inequality'; Calvin *et al.*, 2017), and SSP5 ('fossil-fueled'; Krieglner *et al.*, 2017). The population-weighted degree-days presented in this study combine two RCPs and five SSPs to delineate the areas likely to experience a future increase in energy demand.

After this introduction, Section 2 describes input data and details on the mathematical approach to compute wCDD, wHDD, and wEDD; Section 3 presents and Section 4 discusses the results, focusing on the importance of population weighting in degree-days projections and put special emphasis to the results for SSP5; Section 5 summarizes the outputs and the possible improvements. Additional figures and tables, with results discussed in the main text, are left for Supporting Information.

## 2 | DATA AND METHODS

### 2.1 | Climate data

Daily time series of minimum ( $T_N$ ) and maximum temperature ( $T_X$ ) needed to compute the degree-day indicators over the period 1981–2100 were obtained from the CORDEX datasets. The CORDEX simulations are based on RCMs used to dynamically downscale the GCMs participating to the Coupled Model Intercomparison Project 5 (Taylor *et al.*, 2012): we selected all the currently available combinations of GCMs–RCMs over the 14 CORDEX domains and for two available RCPs: the moderate RCP4.5 (Thomson *et al.*, 2011) and the extreme RCP8.5 (Riahi *et al.*, 2011). Although the computation of threshold-based indices (such as CDD and HDD) would require bias-adjustment of the climate variables (Dosio, 2016; Dosio and Fischer, 2018), only a small subset of CORDEX simulations (and for only very few domains) have been bias-adjusted so far (see: <https://cordex.org/data-access/bias-adjusted-rcm-data/>). In this study, therefore we used the original, non bias-adjusted, CORDEX data.

The simulations used in this study are based on a total of 20 GCMs and 34 RCMs (Table S1), but not all GCMs have been downscaled by all RCMs and the resulting GCM–RCM matrix is somehow sparse and heterogeneous (see, e.g., Dosio *et al.*, 2019 for Africa). Consequently, the number of available simulations strongly depends on the domain, ranging from 16 (South East Asia) to 63 (Africa; Table S2). In addition, as most of the CORDEX domains partially overlap, the actual number of runs available over the macro-regions—including both scenarios RCP4.5 and RCP8.5—ranges from 18 (Antarctica) to 149 (Middle East; Figure S1).

All the indicators and quantities have been calculated for every simulation (most of them available on 0.44° grid) and subsequently interpolated over a common 0.44° grid with the approach used by Spinoni *et al.* (2020): a small discontinuity in the results, due to the heterogeneous number of simulations over CORDEX domains, is present only over the Urals.

To validate the CORDEX simulations over the period 1981–2010, we obtained temperature data from the University of East Anglia's Climate Research Unit (CRU; Harris *et al.*, 2020).

### 2.2 | Heating, cooling, and energy degree-days

Degree-day quantities are usually calculated as the annual (or seasonal) sum of daily temperature values above (CDD) or below (HDD) certain thresholds, to

estimate the energy needed to keep indoor thermal comfort (EEA, 2019). As there is no unique approach (Allen, 1976; Kadioglu and Şen, 1999; Thevenard, 2011), here we decided to follow the one used by the United Kingdom's MetOffice, which derives CDD and HDD with a set of equations based on daily minimum and maximum temperature and base temperatures designed for mid-latitude Europe (Kendon *et al.*, 2016), namely 15.5°C for HDD and 22°C for CDD (Table S3). Because our analyses include global land areas, we computed both CDD and HDD from January to December.

We computed degree-day indicators for each simulation and RCP and we obtained annual series from 1981 to 2100, therefore averaged over 30-year periods, that is, recent past (RP, 1981–2010) and those corresponding to GWLs, obtained following the approach described in, for example, Dosio and Fischer (2018). In details, we firstly derived the global temperature increase from the pre-industrial (1881–1910; see Hawkins *et al.*, 2017) to the RP period (0.96°C according to NASA Goddard's Global Surface Temperature Analysis dataset GISTEMPv4; Hansen *et al.*, 2010). For each GCM (and RCP), we looked for the year corresponding to an additional warming (vs. the RP) which led to 1.5°C (2°C, 3°C, 4°C) from the pre-industrial period. The 30-year period centred on that year corresponds to a GWL of 1.5°C (2°C, 3°C, 4°C) for that run. For each GWL, we used all the RCPs that allow reaching the GWL (also depending on the GCM). Eventually, for each grid point and 30-year period investigated, we obtained the ensemble median (of available simulations) of annual CDD and HDD, after the re-gridding procedure. Finally, we obtained 30-year averaged annual values of EDD as the sum of CDD and HDD.

Our analyses focus on changes in degree-day quantities corresponding to the RP and the GWLs, for example, the change in CDD between the RP and GWL 2°C: such change is defined significant in sign if at least two-third of simulations used agree on the sign of change; significant in magnitude if, in absolute values, is larger than the inter-simulation standard deviation of CDD over RP; if both conditions are fulfilled, the change is robust, and if none, is uncertain.

### 2.3 | Population data and population-weighted degree-days

As input population data, we used the NASA-SEDAC dataset, recently applied in studies on climate change by Jones *et al.* (2018) and Batibeniz *et al.* (2020). We selected version 1.01, downscaled at 1 km from 0.125° resolution (Gao, 2020; Jones and O'Neill, 2020). From NASA-SEDAC projections, we used total residential population data for 2000–2100 consistent with five SSPs (SSP1–SSP5; Jones

and O'Neill, 2016). We assumed that the base year (2000) represents 1981–2010: according to the U.S. Census Bureau (<https://www.census.gov/data.html>), the global population in 2000 is closer to the average population in 1981–2010 (6.5% larger) than the average one in 2000–2010 is (13.1% larger).

Ideally, as climate projections are directly linked to the underlying RCPs, the use of population projections constructed specifically for the RCPs would be recommendable, especially when analysing projections at different periods (e.g., 2080s vs. reference period). However, this study is based on GWLs, which are constructed independently of the RCPs, as discussed earlier. In addition, as the CORDEX simulations are available for all domains for the RCP4.5 and RCP8.5 only, using RCP-specific population projections would have limited our study to the SSP2 and the SSP5, best coupled with, respectively, the RCP4.5 and the RCP8.5 (O'Neill *et al.*, 2017).

In this study, the population weighting of degree-days is achieved by multiplying, for each grid cell, the averaged (over the 30-year period) values of the population by the averaged degree-day values (ensemble median of CORDEX simulations). The results, firstly on regular grids (0.44°), are therefore aggregated over macro-regions (Figure S2) and continents for GWLs from 1.5°C to 4°C.

To do that, population data are aggregated from 1 km resolution to the 0.44° CORDEX one and to macro-regional and continental scales (Figures S3 and S4). As population data are provided at 10-year temporal resolution, for each grid point and SSP we first reconstructed the annual population series and, then, we averaged the 30-year values corresponding to the selected GWL. We performed such calculations for the viable combinations of SSPs–GWLs: SSP1 limits to GWL 1.5°C, SSP2 to 2°C, SSP4 to 3°C, and both SSP3 and SSP5 to 4°C (van Vuuren and Carter, 2014; O'Neill *et al.*, 2016; Riahi *et al.*, 2017).

Population projections are not free from uncertainties (Raftery *et al.*, 2014; Azose *et al.*, 2016), but the NASA-SEDAC's ones—at the spatial resolution selected—are not provided with an estimate of errors. Consequently, we assumed that the uncertainties in the population-weighted degree-day projections derive from climate components only (see Section 3.2).

### 3 | RESULTS

#### 3.1 | Evolution of CDD, HDD, and EDD in 21st century

Cooling and heating degree-days directly depend on temperature, so the projected warming of the 21st century is expected to result in corresponding increase of CDD and

decrease of HDD. Such projected temperature increase shows heterogeneous spatial patterns, with largest values over high latitudes in the Northern Hemisphere and smallest over tropical and equatorial latitudes, being this difference larger with higher GWLs (Table S4). For example, according to the CORDEX ensemble, the average temperature increase from 1981–2010 to GWL 4°C in Alaska is approximately twice that in the Caribbean region.

The patterns of temperature projections, together with daily variability, are the main drivers of degree-day projections (Figure 1). CDD, whose values are null or show negligible changes over cold or very cold regions, show the largest increase in Amazonia, most of Africa, southern Asia, and northern Australia. At 1.5°C warming, the increase in CDD is robust only over Australia, but at higher GWLs it is robust over progressively larger areas and, at GWL 4°C, it is robust everywhere but the Tibetan Plateau and bordering areas between central United States and Canada. As expected, HDD show an opposite tendency, with the largest decrease over cold and very cold regions (at high latitudes in both Hemispheres and over the Tibetan Plateau). The decrease in HDD is generally not robust at GWL 1.5°C, but becomes progressively robust with increasing GWL, and, at GWL 4°C, it is robust everywhere excluding equatorial and tropical latitudes in South America, Africa, southern Asia, and northern Australia. A possible explanation for the not robust change in CDD and HDD at GWL 1.5°C is that the corresponding change in temperature almost everywhere lies in the range of variability of 1981–2010 (Hawkins *et al.*, 2016).

Regarding EDD, they show almost no change at GWL 1.5°C. The exceptions are very cold regions, with a decrease in EDD due to a decrease in HDD, and Amazonia, the Sahel, and northeastern Australia (the only part of the World where the change is robust at 1.5°C warming), with an opposite increase in EDD driven by an increase in CDD. The areas showing a decrease in EDD at GWL 1.5°C, show larger decreases at GWL 2°C and this is also valid for the areas showing increases. The decrease in EDD is robust only in northeastern North America and Eastern Europe, due to a decrease in HDD and negligible change in CDD. Instead, the increase in EDD is robust in central Brazil (decrease in CDD and no change in HDD) and in most of Australia (where an increase in CDD overbalances a decrease in HDD).

At GWL 3°C, the change in EDD is likely to be robust everywhere except parts of the United States, Argentina, central Asia, China, and southern Australia, and at GWL 4°C the areas of non-robust change are further reduced. At high GWLs there is a latitudinal belt—slightly larger than the tropics—where EDD are projected to increase (robust increase in CDD and almost negligible decrease in HDD), with the exceptions of the Andes (decrease due

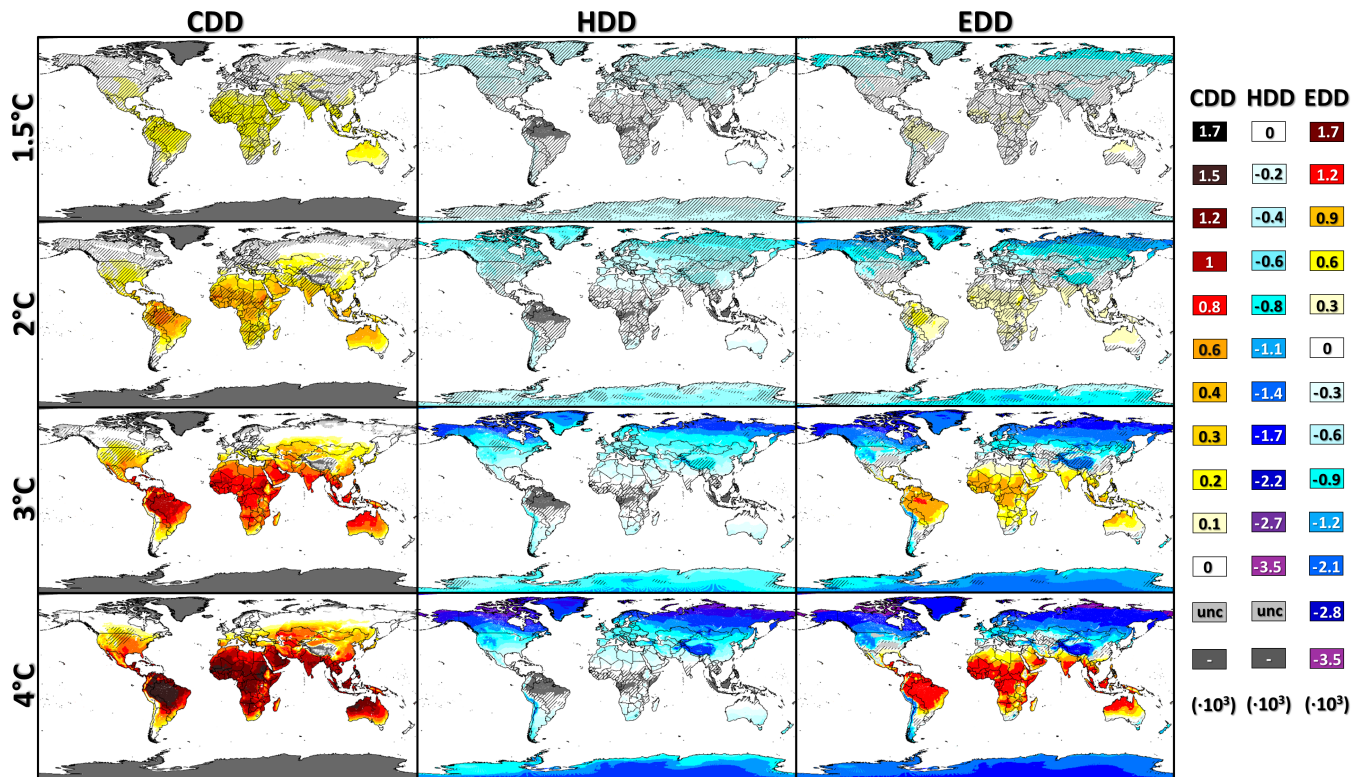


**FIGURE 1** Cooling, heating, and energy degree-days change from 1981–2010 to four GWLs, expressed as the average annual sum over the corresponding 30-year periods (in  $10^3$  units). Colour-scale values represent a robust change, superimposed dashed lines a change significant in sign only, light grey a not significant change. Dark grey refers to null degree-day quantity in any period. CDD, cooling degree-days; EDD, energy degree-days; GWLs, global warming levels; HDD, heating degree-days [Colour figure can be viewed at [wileyonlinelibrary.com](http://wileyonlinelibrary.com)]

to decrease in HDD at high elevations) and Ethiopia (no change due to small change in both CDD and HDD). Conversely, mid and high latitudes in the Northern Hemisphere, the Andes and southern Argentina, Tibetan Plateau, and Antarctica show robust decrease in EDD at high GWLs, with the largest decrease (arctic Canada) twice as wide as the largest increase (northern Amazonia). Mid-latitudes in the Northern Hemisphere, as the Mediterranean region, are projected to experience both robust decrease in HDD and robust increase in CDD, with the latter progressively overbalancing the former with increasing warming.

Overall, EDD are projected to significantly increase over approximately 47% of land at GWL 1.5°C and such value slightly increases to exceed 50% only at GWL 4°C (Table 1). Only a small fraction of land (3.5%, approximately 5 million  $\text{km}^2$ ) is projected to turn from negative to positive balance between an increase in CDD and a decrease in HDD from GWL 1.5°C to 4°C. The regions with the largest enlargement of areas with significant increase in EDD, from lowest to highest GWLs, are the Mediterranean region (+16.8%) and southern Australia (+15.7%). Including population in the analyses is crucial, as, for example, many areas where EDD are projected to

change are currently totally or almost uninhabited (Figure 1): the Arctic, Antarctica, and high latitudes of North America, Europe, and Asia (decrease in EDD), or the Sahara and central Australia (increase in EDD).

At continental scale (Figure 2), the extent of areas with increase in EDD becomes larger with increasing GWL, but the change—either positive or negative—tends to become robust (instead of only significant in sign) for larger areas. Globally, the robust increase (decrease) in EDD moves from approximately 5% (3%) at GWL 1.5°C to approximately 50% (45%) at GWL 4°C. In the Northern Hemisphere, the areas with a decrease in EDD (approximately 53% at GWL 4°C) are larger than those with an increase in EDD, and the situation is reversed for the Southern Hemisphere (approximately 68% of areas with increase in EDD at GWL 4°C).

### 3.2 | Uncertainty in degree-day projections

Before analysing the projected population-weighted degree-days, we performed a three-step analysis on degree-day projections to detect the areas with largest uncertainties. As mentioned in Section 2.3, in this study

**TABLE 1** Macro-regional area (%) with projected significant (in sign) increase in energy degree-days (EDD)

Region	EDD > 0			
	1.5°C	2°C	3°C	4°C
ALA	0.0	0.0	0.0	0.0
NEC	0.0	0.0	0.0	0.0
GIC	0.0	0.0	0.0	0.0
NWN	0.0	0.0	0.0	0.0
SWN	10.7	11.8	12.6	15.4
CAN	22.2	21.9	24.9	28.9
ENA	15.6	17.8	20.9	22.9
CAM	72.0	72.8	76.6	80.9
CAR	100.0	100.0	100.0	100.0
NWS	74.3	75.8	79.5	82.2
SAM	90.1	90.2	91.0	91.1
SSA	0.0	0.0	0.0	0.0
SWS	4.2	4.5	5.7	7.5
SES	58.0	58.0	63.1	66.0
AMZ	99.8	99.9	100.0	100.0
NEB	100.0	100.0	100.0	100.0
NEU	0.0	0.0	0.0	0.0
CEU	0.0	0.0	0.0	0.0
MED	27.8	31.9	39.2	44.6
SAH	99.5	99.9	100.0	100.0
WAF	100.0	100.0	100.0	100.0
NEAF	89.1	89.8	93.2	95.0
CEAF	95.7	97.0	98.6	99.3
SWAF	79.6	81.3	86.4	90.0
SEAF	82.3	84.0	87.9	89.3
CAF	100.0	100.0	100.0	100.0
NEA	0.0	0.0	0.0	0.0
NWA	0.0	0.0	0.0	0.0
WAS	52.2	54.7	58.5	60.3
CAS	8.5	14.0	19.4	21.3
TIB	0.7	0.8	0.9	0.9
EAS	11.7	15.3	18.5	22.7
SAS	82.8	84.2	85.9	86.3
SEA	99.5	99.5	99.9	100.0
NAU	98.8	99.2	99.5	99.6
SAU	29.2	36.2	41.7	44.9
ANT	0.0	0.0	0.0	0.0
ARCO	0.0	0.0	0.0	0.0
WORLD	46.7	47.6	49.1	50.2

Note: See Figure S2 for the macro-regions.

we assumed that only the climate component is responsible for the uncertainties in the final outputs.

Firstly, we evaluated how the results based on the CORDEX simulations perform when applied to the recent past. We compared the average annual CDD and HDD in 1981–2010 obtained using the CORDEX ensemble with those obtained using the CRU's observational dataset (Figure S5): compared to observations, models lead to smaller CDD values at tropical latitudes (but larger over Amazonia), to smaller HDD values at high latitudes in the Northern Hemisphere, and to larger HDD values over the Tibetan Plateau, with a discontinuity over the Urals. Such discrepancies are larger than 10% only on 7.1% of global lands for CDD and 3.8% for HDD.

Secondly, we evaluated the inter-model spread derived by the use of a large ensemble of simulations, calculated as the inter-model standard deviation of the change between the selected GWL and 1981–2010. At GWL 2°C (Figure S6) the spread for CDD is largest, in absolute value, over the central-northern United States, Amazonia, Eastern Europe, and northwestern Australia, and for HDD over Siberia and Antarctica (mostly uninhabited). As expected, in percentage values the spread for CDD is larger than that for HDD, especially in cold areas with low CDD values. Table 2 shows the inter-model spread of EDD, which is larger than the absolute change at every GWL only for few regions, namely central North America, southwestern South America, the Mediterranean region, and southern Australia.

Thirdly, we evaluated whether the CORDEX ensemble concurs on projected increase (or decrease) in EDD. We calculated the percentage of area with more than two-thirds of simulations agreeing on the sign of change. Table 2 shows that the change in EDD is significant in sign in more than 85% of all macro-regions but Central North America, with such a region standing out as the one with most uncertain tendencies also from Figure 1.

Based on these analyses, it is likely that the population-weighted degree-day projections (discussed in the following sections) are likely to show larger uncertainties when based on CDD than HDD. The areas with the largest uncertainties are the central United States, Amazonia, southern South America, Eastern Europe, the Mediterranean region, the Sahel, tropical southern Asia, and southern Australia. However, considering population density larger than 1 person/km<sup>2</sup>, less than 4% of global areas shows inter-model spread larger than 10%—at any GWL—in at least one of the degree-day indicators. Moreover, the models agreement in the sign of change is significant over 98% of global lands and for all GWLs (over 99% excluding the sparsely populated areas).

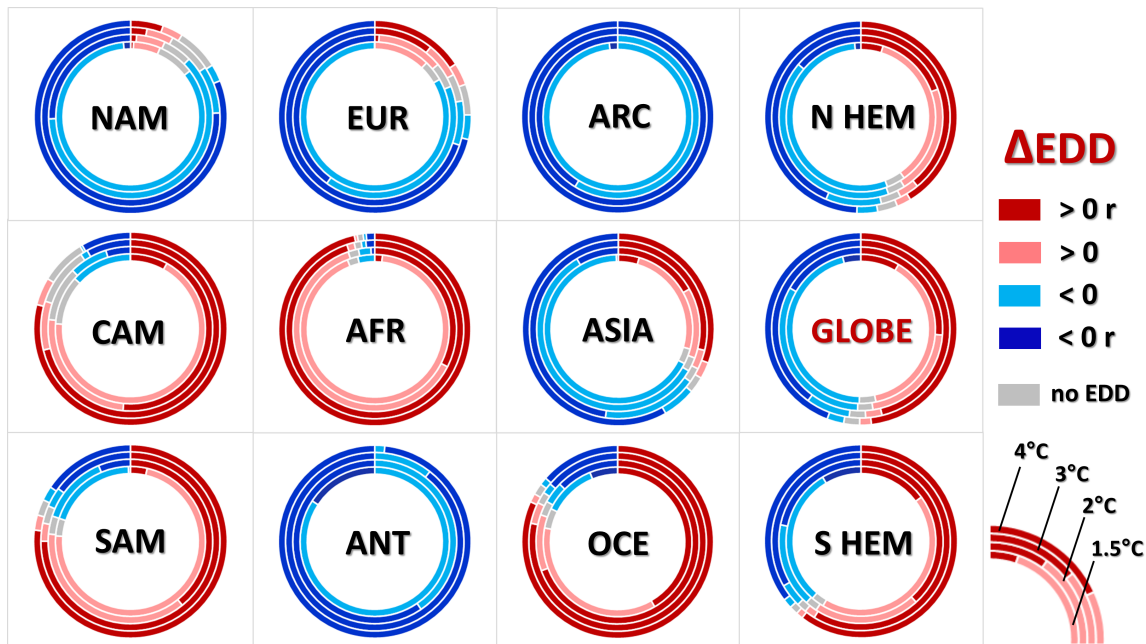


**FIGURE 2** Area (%) projected to see a change in energy degree-days from 1981–2010 to four GWLs. Robust change ( $r$ ) in dark red and blue, significant in sign in light blue and pink, not significant in grey. GWLs, global warming levels; EDD, energy degree-days. Note: See Figure S2 for the continents [Colour figure can be viewed at [wileyonlinelibrary.com](http://wileyonlinelibrary.com)]

As additional validation, we compared the degree-day projections discussed in this study with the corresponding ones computed using bias-adjusted temperature data from the 11 (22 considering the 2 RCPs) EURO-CORDEX simulations applied in Spinoni *et al.* (2018). We highlight that the number of the non bias-adjusted runs is larger (approximately four times in Northern and Central Europe and six times in Southern Europe) than the number of bias-adjusted ones. As the spatial resolutions are different ( $0.11^\circ$  for bias-adjusted simulations vs.  $0.44^\circ$  for those used here), we performed the comparisons using averages within the borders of three European macro-regions, namely Northern Europe, Central Europe, and Mediterranean Region (see Figure S2).

Figure S7 shows an excellent agreement between the two datasets regarding HDD: considering all the GWLs and the three macro-regions, the discrepancy remains smaller than 1% at  $1.5^\circ\text{C}$  GWL, only slightly increasing with GWL, but never exceeding 4%. Regarding CDD, the agreement decreases with increasing GWL, showing notable differences at  $4^\circ\text{C}$  warming in Northern Europe, though this also depends on the large increase in percentage values (but small in absolute values) due to typically low (or very low) annual CDD at high latitudes. Excluding from the averages the sparsely populated areas ( $<1$  person/ $\text{km}^2$ ), the discrepancy between the two datasets regarding CDD exceeds 20% only over Northern Europe and for high GWLs ( $3^\circ\text{C}$  and  $4^\circ\text{C}$ ).

### 3.3 | Population-weighted projections of HDD, CDD, and EDD

In 1981–2010, western Africa, India, eastern China, and southeastern Asia showed the largest population-weighted CDD values (wCDD; Figure 3). With increasing GWL, the largest increase in wCDD is likely to occur in tropical Africa, India, and Iraq, while in the Southern Hemisphere the projections show (very) small change (Figure S7). At the highest GWL (specific for each SSP) eastern China is the only area with a projected decrease in wCDD, and only with SSP4 (at GWL  $3^\circ\text{C}$ ), due to projected population decrease with SSP4. At GWL  $4^\circ\text{C}$  (SSP3 and SSP5), the regions with the largest projected change are located in sub-Saharan Africa, excluding regions with very small wCDD in 1981–2010 and therefore subjected to enormous percentage increase (Figure 3 and Table S4).

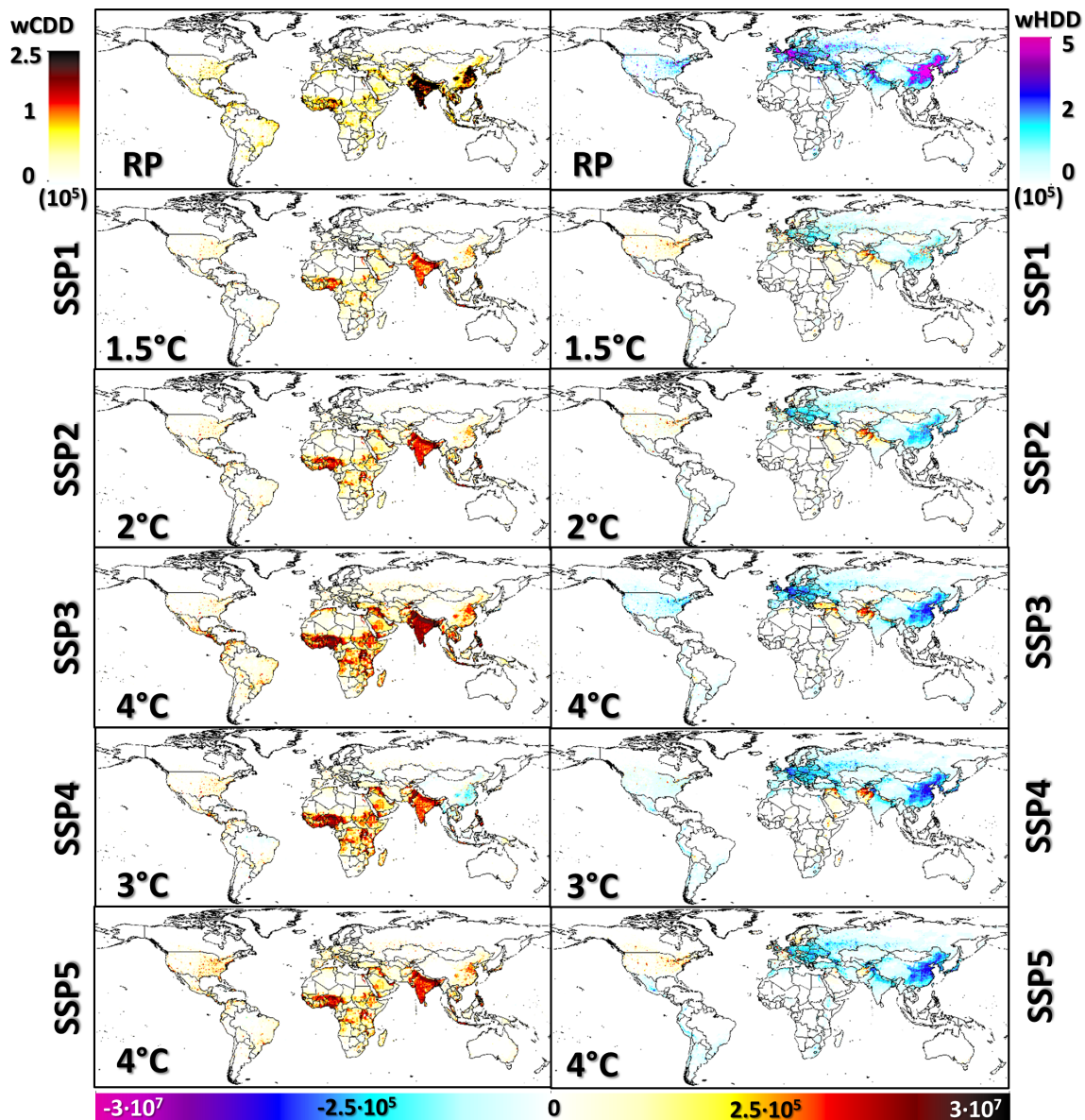
Regarding population-weighted HDD (wHDD) the largest values in 1981–2010 are located in the northeastern United States, Europe, northern India, and eastern China (Figure 3), with the latter two regions showing very high values for both wCDD and wHDD because of very high population density. In the 21st century, Europe and eastern China show the largest projected decrease in wHDD (especially with SSP3, SSP4, and SSP5), whereas Afghanistan and Pakistan the largest increase (Figure 3 and Figure S8). Even at the highest GWL, most of the Southern Hemisphere shows very small changes in wHDD for all SSPs (Figure 3). The Middle East shows

TABLE 2 Left: Ensemble median change EDD, averaged at macro-regional scale and expressed in percentage, between GWLs and 1981–2010

% Region	$\Delta$ (EDD)				$\sigma$ (EDD)				Sign $\Delta$ (EDD)			
	1.5°	2°	3°	4°	1.5°	2°	3°	4°	1.5°	2°	3°	4°
ALA	-6.1	-11.0	-18.9	-27.4	1.7	2.3	3.6	4.5	100.0	100.0	100.0	100.0
NEC	-5.4	-10.2	-18.3	-26.0	1.8	2.9	4.8	6.0	100.0	100.0	100.0	100.0
GIC	-3.5	-6.4	-11.6	-16.2	1.4	1.8	2.8	3.0	100.0	100.0	100.0	100.0
NWN	-5.8	-10.9	-17.3	-25.0	2.7	4.0	6.8	8.8	99.6	99.8	97.0	96.6
SWN	-4.4	-7.7	-11.7	-13.8	4.0	6.1	10.2	13.1	87.6	93.0	90.7	91.8
CNA	-1.5	-3.6	-4.9	-5.1	4.0	6.4	10.7	13.4	69.2	78.0	71.5	75.8
ENA	-3.0	-5.1	-7.8	-10.5	3.0	4.9	8.7	11.3	87.4	89.7	86.3	87.2
CAM	9.0	17.9	37.1	59.1	6.0	10.4	17.6	22.6	87.5	87.3	87.5	91.1
CAR	16.8	31.1	56.7	81.6	3.8	5.0	7.7	9.1	100.0	100.0	100.0	100.0
NWS	9.3	17.8	38.8	60.6	5.4	8.7	15.8	21.2	93.9	93.7	95.5	96.7
SAM	11.9	21.7	43.8	67.4	4.3	6.4	12.5	16.3	99.1	99.3	99.9	99.8
SSA	-4.9	-8.6	-15.4	-21.1	1.7	2.1	2.5	3.6	100.0	100.0	100.0	100.0
SWS	-5.5	-8.8	-11.7	-11.5	7.0	11.1	20.0	26.6	97.2	96.6	95.8	95.6
SES	4.1	7.9	19.3	33.5	4.4	6.5	12.6	16.9	88.5	89.5	90.0	91.7
AMZ	15.0	26.6	51.3	74.6	4.7	6.9	13.0	16.7	99.8	99.9	100.0	100.0
NEB	17.5	32.1	62.1	93.7	6.0	8.2	15.5	19.5	100.0	100.0	100.0	100.0
NEU	-7.3	-12.6	-20.8	-27.8	2.6	3.2	4.6	5.1	100.0	100.0	100.0	100.0
CEU	-6.6	-10.5	-18.2	-24.1	3.3	3.9	6.6	8.9	100.0	100.0	100.0	100.0
MED	-2.7	-3.2	-2.4	0.7	3.5	5.0	8.1	11.0	91.0	89.8	89.8	89.4
SAH	8.0	14.5	29.8	45.0	3.8	5.0	8.7	11.2	99.5	99.9	100.0	100.0
WAF	13.4	23.7	44.7	64.8	3.7	4.8	9.3	12.3	100.0	100.0	100.0	100.0
NEAF	11.1	20.4	42.3	62.4	4.8	7.0	12.5	17.1	96.8	96.6	96.9	97.2
CEAF	16.3	29.2	63.5	94.8	6.8	10.5	17.6	23.9	97.5	98.0	99.2	99.5
SWAF	9.3	18.3	41.7	75.0	7.7	12.6	23.7	33.5	90.6	90.8	94.7	97.0
SEAF	12.9	24.6	54.7	89.4	7.4	10.8	18.5	26.0	94.6	95.2	96.8	96.9
CAF	15.7	27.4	54.0	79.3	4.3	5.9	11.6	14.6	100.0	100.0	100.0	100.0
NEA	-5.8	-10.1	-17.6	-24.0	1.6	2.1	3.0	3.7	100.0	100.0	100.0	100.0
NWA	-6.6	-11.4	-19.6	-25.5	2.5	2.9	4.2	4.8	100.0	100.0	100.0	100.0
WAS	1.1	2.8	7.1	12.8	2.9	3.7	5.8	7.6	92.2	91.8	93.5	93.1
CAS	-3.3	-4.8	-7.3	-8.4	2.7	3.3	4.8	6.1	88.8	90.4	91.9	89.7
TIB	-4.1	-7.0	-12.5	-16.7	1.9	2.2	3.4	4.3	99.8	99.8	99.9	99.9
EAS	-2.9	-4.4	-5.7	-5.8	2.6	3.3	5.2	7.0	93.4	94.5	92.8	93.5
SAS	7.3	13.5	27.6	42.8	3.7	5.0	9.4	12.3	96.7	97.7	98.8	98.9
SEA	15.2	26.6	50.6	74.5	4.1	5.6	10.1	13.7	99.7	99.7	99.9	100.0
NAU	11.6	19.7	36.2	56.0	4.7	5.5	9.6	14.3	99.3	99.6	99.8	99.9
SAU	-5.3	-7.0	-5.6	-0.8	5.8	7.3	11.0	15.6	87.5	91.7	93.8	94.2
ANT	-1.5	-3.0	-5.2	-7.5	0.6	0.8	1.1	1.5	100.0	100.0	100.0	100.0
ARCO	-5.4	-9.6	-17.6	-26.1	2.0	3.1	5.2	6.9	100.0	100.0	100.0	100.0

Note: Centre: Standard deviation of the ensemble mean change in EDD, in percentage values (in italics: Standard deviation larger than mean change in absolute values). Right: Percentage of each macro-region with at least two-thirds of the simulations agreeing on the sign of the ensemble median change. Abbreviation: EDD, energy degree-days.





**FIGURE 3** Population-weighted cooling (left) and heating (right) degree-days for 1981–2010 (RP) and projected change (colour-scale below the panels) between RP and four GWLs following five SSPs. GWLs, global warming levels; RP, recent past; SSPs, socio-economic scenarios; wCDD, weighted cooling degree-days; wEDD, weighted energy degree-days; wHDD, weighted heating degree-days [Colour figure can be viewed at [wileyonlinelibrary.com](http://wileyonlinelibrary.com)]

different tendencies (increase with SSP1–SSP4 and decrease with SSP5) and so do the northeastern United States (increase with SSP1, SSP2, and SSP5, no change with SSP3, and decrease with SSP4; Figure S8 and Table S5).

The population-weighted EDD (wEDD; Figure 4) show largest values in Europe, India, and eastern China in 1981–2010; according to all SSPs, they are projected to decrease in Europe and eastern China (excluding SSP1 and low GWLs for other SSPs) and to increase in tropical Africa, the Middle East, and India. The increase is the largest over tropical latitudes, especially in western and

central-eastern Africa where, for SSP3, wEDD are likely to be 10 times larger at GWL 4°C than in 1981–2010 (Table S6), due to both steep population increase and strong warming. In the United States, wEDD are overall likely to increase with all SSPs except for SSP3 (decrease). In North America, the SSP4 shows an interesting feature: contrasting tendency between large cities (wEDD projected to increase) and the countryside (decrease), possibly because of the specific country-scale urbanization projections included in the SSPs (Jiang and O'Neill, 2017; Gao and O'Neill, 2020). Detailed analyses on wEDD projections for large cities are left for further studies.

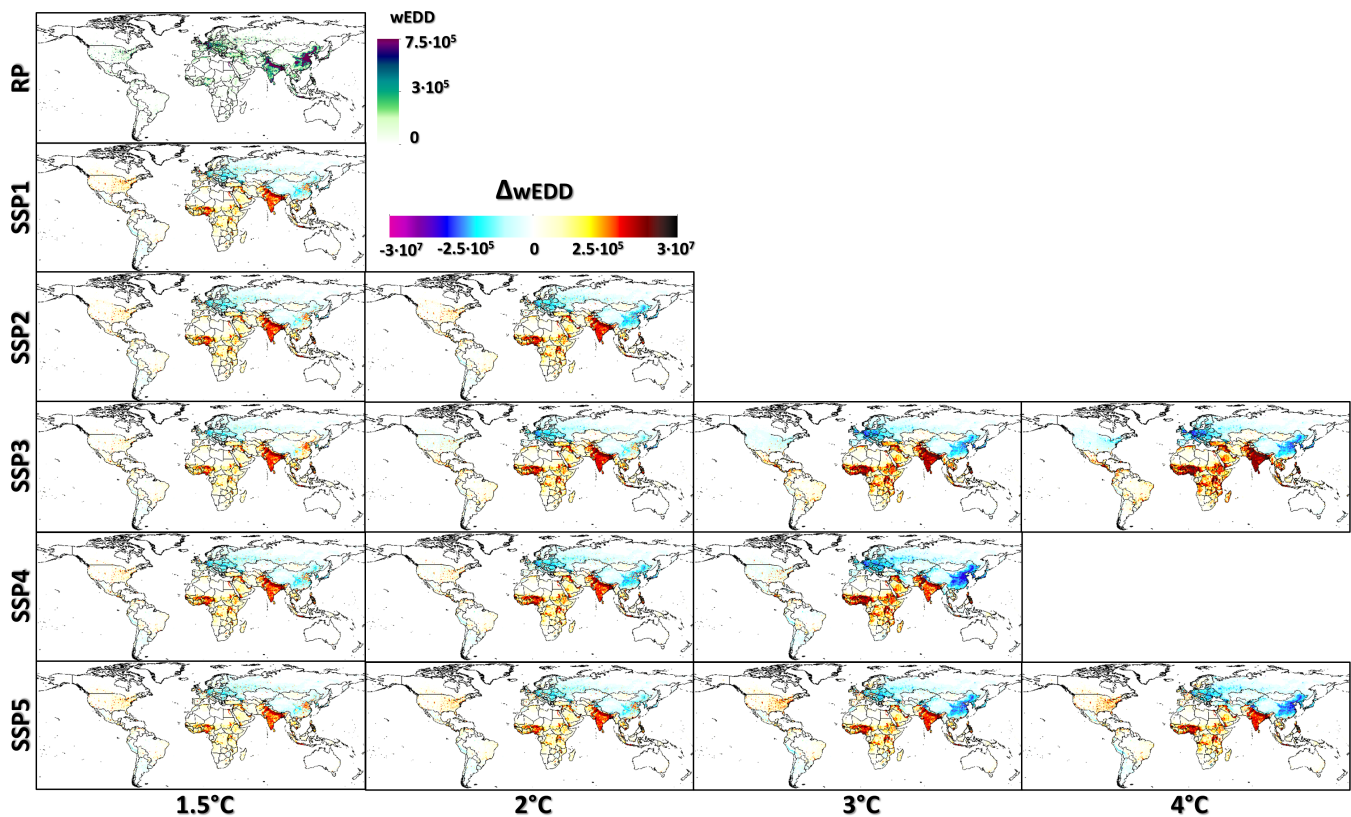


**FIGURE 4** Population-weighted energy degree-days for 1981–2010 (RP) and projected change at four GWLs following five SSPs. GWLs, global warming levels; RP, recent past; SSP, socio-economic scenarios; wEDD, weighted energy degree-days [Colour figure can be viewed at [wileyonlinelibrary.com](http://wileyonlinelibrary.com)]

In a World following SSP1 or SSP2, all population-weighted degree-day indicators are likely to moderately increase in all continents (Table 3 and Figure S9), excluding wHDD in South America, Europe (SSP2 only), and Asia, where the decrease is very small (down to  $-10\%$  for Asia with SSP2). With the more severe SSP3, SSP4, or SSP5, wCDD are likely to become at least twice as large as in 1981–2010 in all continents but South America ( $+79\%$  for SSP4). Instead, wHDD show opposite tendencies depending on the SSP in North and Central America, Africa, and Oceania. Combining wCDD and wHDD, wEDD are likely to increase with any SSP and in all continents, excluding North America (decrease with SSP3) and Europe (decrease with SSP3 and SSP4), mostly due to population decrease or non-continuous increase.

### 3.4 | The special case of fossil-fuelled development (SSP5)

To focus on a special SSP, we chose the SSP5 because it is best coupled with climate scenario RCP8.5 (Jones and O'Neill, 2016) and more than half climate simulations used in this study are based on the RCP8.5. Moreover, we

wanted to investigate on the impacts of severe climate change on degree-days, and the RCP8.5, is regarded as the most severe climate scenarios of its generation (Sillmann *et al.*, 2013; Gattuso *et al.*, 2015; Hausfather and Peters, 2020). In details, the RCP8.5 projects a continuous rise of emissions during the 21st century and the SSP5 foresees a World based on 'fossil-fuelled development' with continuous growth of economy but population decline after peaking around 2050 (Bauer *et al.*, 2017; Kriegler *et al.*, 2017; Samir and Lutz, 2017).

Figure 5 shows that, with a SSP5-based future, wCDD are likely to increase everywhere excluding uninhabited regions. As the warming increases, wHDD oppositely tend to decrease in all inhabited regions excluding central and eastern North America, northeastern Canada, northern Europe, and southern Australia. Consequently, wEDD are projected to increase in all regions with not negligible population, excluding southwestern South America, central Europe, Tibetan Plateau, and northeastern, northwestern, and eastern Asia.

In a World which follows RCP8.5-SSP5, most regions are likely to see an increased need of energy to cool and heat the environments, partly because in such regions the increase in CDD will outbalance the decrease in

**TABLE 3** Average annual population-weighted cooling (wCDD), heating (wHDD), and energy degree-days (wEDD) for 1981–2010 (RP, in 10<sup>6</sup> units) and change between RP and GWLs (in %) following different SSPs

Ind	GWL	1.5°			2°			3°			4°				
		RP	SSP1	SSP2	SSP3	SSP4	SSP5	SSP2	SSP3	SSP4	SSP5	SSP3	SSP4	SSP5	
wCDD	NAM	60.5	87.1	68.1	48.5	61.6	68.2	113.0	70.9	91.4	115.9	99.1	144.2	274.8	399.9
	CAM	50.7	40.0	59.5	65.6	55.8	41.6	86.3	125.7	80.8	60.8	237.4	111.8	71.8	349.3
	SAM	99.5	51.5	63.0	63.4	56.8	49.1	89.4	113.9	77.7	72.0	202.3	79.1	96.2	121.1
wHDD	EUR	75.8	74.9	82.5	78.9	75.2	67.8	121.4	137.4	105.0	101.5	254.6	145.8	176.2	374.4
	AFR	313.2	154.6	183.0	152.9	211.4	123.4	301.7	319.7	314.8	182.2	658.7	705.2	315.4	947.8
	ASIA	1,580.9	61.3	72.1	69.0	68.7	56.3	98.4	118.6	90.6	77.9	200.6	105.3	99.0	275.0
wEDD	OCE	3.0	117.5	96.4	69.3	88.7	90.8	161.7	110.3	132.4	154.2	155.9	205.4	357.6	520.4
	WORLD	2,197.5	74.8	87.4	80.3	88.2	65.9	127.8	146.4	122.2	93.9	265.7	192.2	136.8	372.0
	NAM	322.3	40.4	24.5	9.0	19.8	25.5	27.0	-0.3	14.0	29.9	-22.8	-2.1	54.2	44.5
wHDD	CAM	24.9	22.8	34.4	33.1	30.3	20.7	21.8	38.8	12.9	5.8	32.1	-26.8	-26.8	5.6
	SAM	60.5	-0.1	8.8	10.7	5.4	-0.4	-2.2	12.6	-6.4	-11.2	3.2	-36.3	-36.4	-7.8
	EUR	1,113.6	4.9	-0.8	-4.9	-4.2	0.9	-6.2	-13.7	-11.8	-1.9	-30.1	-35.5	-4.3	-41.4
wEDD	AFR	41.4	31.5	39.4	27.4	46.2	20.1	32.3	35.2	32.4	7.1	23.2	18.1	-17.7	1.0
	ASIA	2,113.3	-1.0	2.9	5.2	-0.4	0.7	-10.0	-0.8	-10.9	-7.9	-17.0	-43.6	-34.3	-27.7
	OCE	7.2	61.6	40.6	16.6	35.5	38.8	44.5	7.7	27.2	42.4	-20.6	6.5	66.0	36.7
wEDD	WORLD	3,684.3	5.1	4.5	3.1	1.1	3.3	-4.7	-3.7	-8.2	-2.5	-20.4	-36.5	-17.0	-29.7
	NAM	396.8	48.1	31.7	15.6	26.7	32.6	41.0	11.3	26.6	44.0	-3.4	21.2	89.3	98.6
	CAM	77.0	34.2	51.2	54.8	47.4	34.6	64.5	96.4	57.9	42.1	168.6	65.5	38.6	235.5
wEDD	SAM	161.7	32.0	42.5	43.5	37.3	30.3	55.1	75.9	46.2	40.8	127.3	35.6	46.1	178.9
	EUR	1,201.8	10.0	5.1	1.0	1.4	5.7	3.2	-2.9	-3.1	6.1	-11.2	-23.3	8.2	-14.4
	AFR	359.0	139.5	165.5	137.6	191.3	110.8	269.2	285.4	280.7	161.0	581.3	621.5	274.7	832.0
wEDD	ASIA	3,742.4	25.6	32.5	32.5	29.2	24.4	36.3	50.3	32.4	28.7	76.3	20.1	22.9	101.7
	OCE	10.3	78.9	57.7	32.7	51.9	54.8	79.9	38.5	59.0	76.2	32.8	67.0	154.9	21.4
	WORLD	5,964.0	31.2	35.6	32.0	33.7	26.8	45.0	52.5	40.6	33.7	86.5	48.8	40.7	118.3

Note: In bold, the highest GWL for each SSP.

Abbreviations: GWL, global warming levels; RP, recent past; SSP, socio-economic scenarios; wCDD, weighted cooling degree-days; wHDD, weighted heating degree-days.

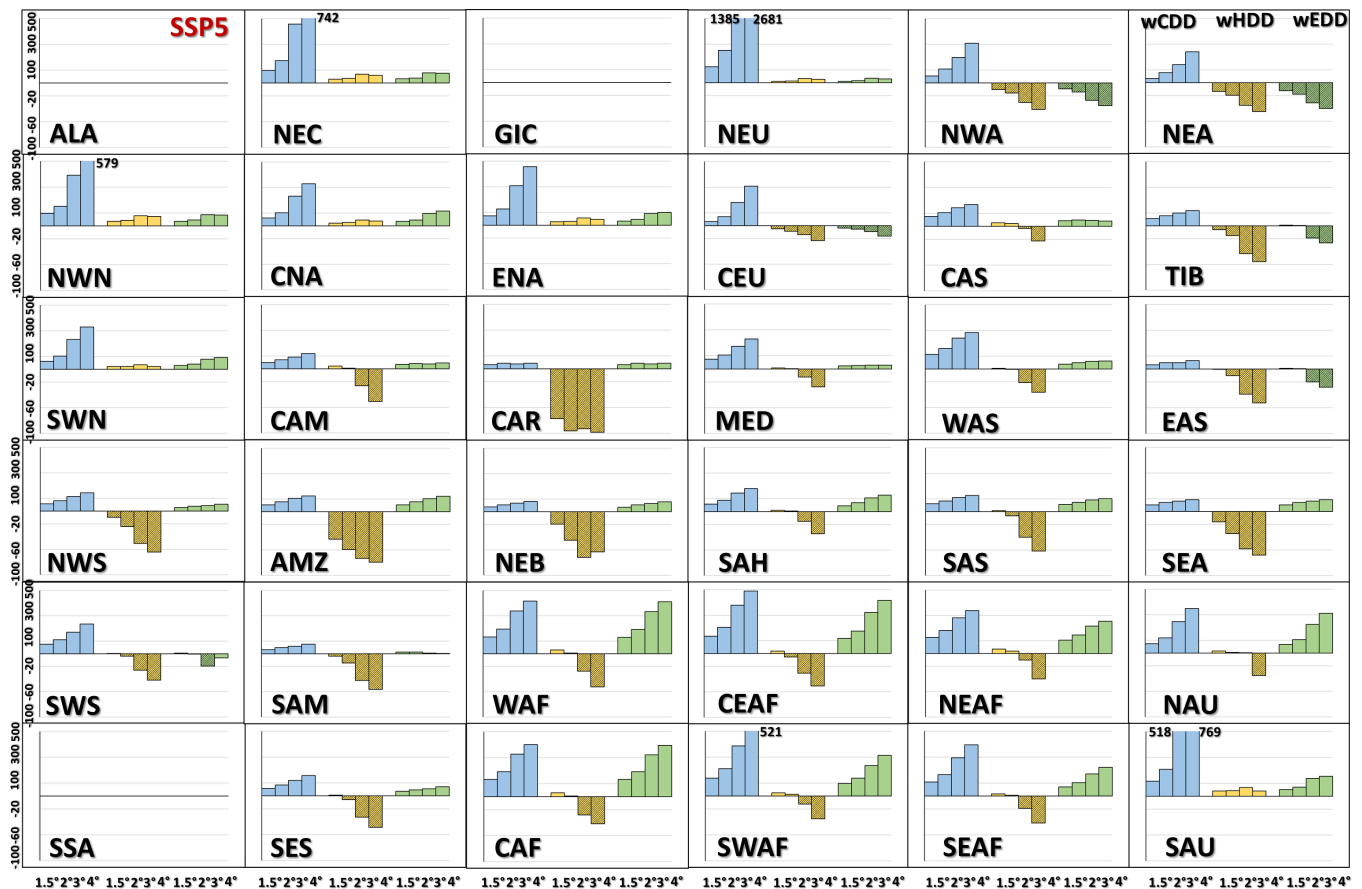


FIGURE 5 Macro-regional cooling (light blue), heating (orange), and energy (green) degree-days projected change (%) from 1981–2010 to four GWLs and following the SSP5. wCDD, weighted cooling degree-days; wHDD, weighted heating degree-days; wEDD, weighted energy degree-days; GWLs, global warming levels; SSP, socio-economic scenario.

Note: See Figure S2 for macro-regions [Colour figure can be viewed at [wileyonlinelibrary.com](https://onlinelibrary.wiley.com)]

HDD, but also because population at the end of the 21st century is indeed larger than recent past, though the global increase is smaller than with SSP2, SSP3, and SSP4 (Figure S4). The exceptions are few and, excluding southwestern South America, are regions at mid-high latitudes in Eurasia where the decrease in HDD is larger than the increase in CDD and population is projected to decrease during the 21st century. Globally, the increase in wEDD with the combination RCP8.5–SSP5 increases from 27% at GWL 1.5°C, to 34%, 41%, and 44% respectively, at GWLs 2°C, 3°C, and 4°C (Table S4).

## 4 | DISCUSSION

From a climatological point of view, the effect of progressive global warming on degree-day quantities results in global net balance, with approximately half of the World's land areas with increasing EDD and half with decreasing EDD in the 21st century (Figure 2). Thus, if we unrealistically assumed that every place in the World

will see current population unchanged in the future, we would conclude that projected climate change will result in a balanced increase in CDD and decrease in HDD, because areas with projected robust increase and those with projected decrease in EDD include approximately the same population.

Population is indeed projected to be higher in 2100 than currently, but such increase will be continuous at global scale with SSP3 only, with other SSPs projecting a stagnation after 2060 (SSP2 and SSP4) or a slow decrease after 2050 (SSP1 and SSP5). Each continent follows specific evolution with each SSP (Figure S4), so the spatial distribution and the time evolution of population are fundamental to estimate if and where we will need more or less energy to heat and cool the environments during the 21st century.

According to Figure 6, the global total of wCDD will increase with any SSP, from 75% with SSP1 (GWL 1.5°C) to 372% with SSP3 (GWL 4°C), which represents the worst-case scenario also due to the continuous population increase—on average—on both Hemispheres. Globally, wHDD will slightly increase with SSP1 (5% at GWL 1.5°)

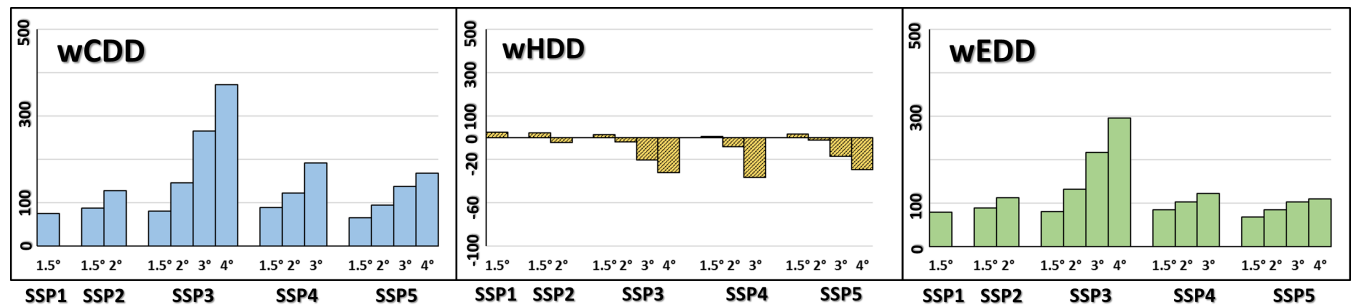


**FIGURE 6** Global cooling (light blue), heating (orange), and energy (green) degree-days projected change (%) from 1981–2010 to four GWLs and following five SSPs. GWLs, global warming levels; SSPs, socio-economic scenarios; wCDD, weighted cooling degree-days; wEDD, weighted energy degree-days; wHDD, weighted heating degree-days [Colour figure can be viewed at wileyonlinelibrary.com]

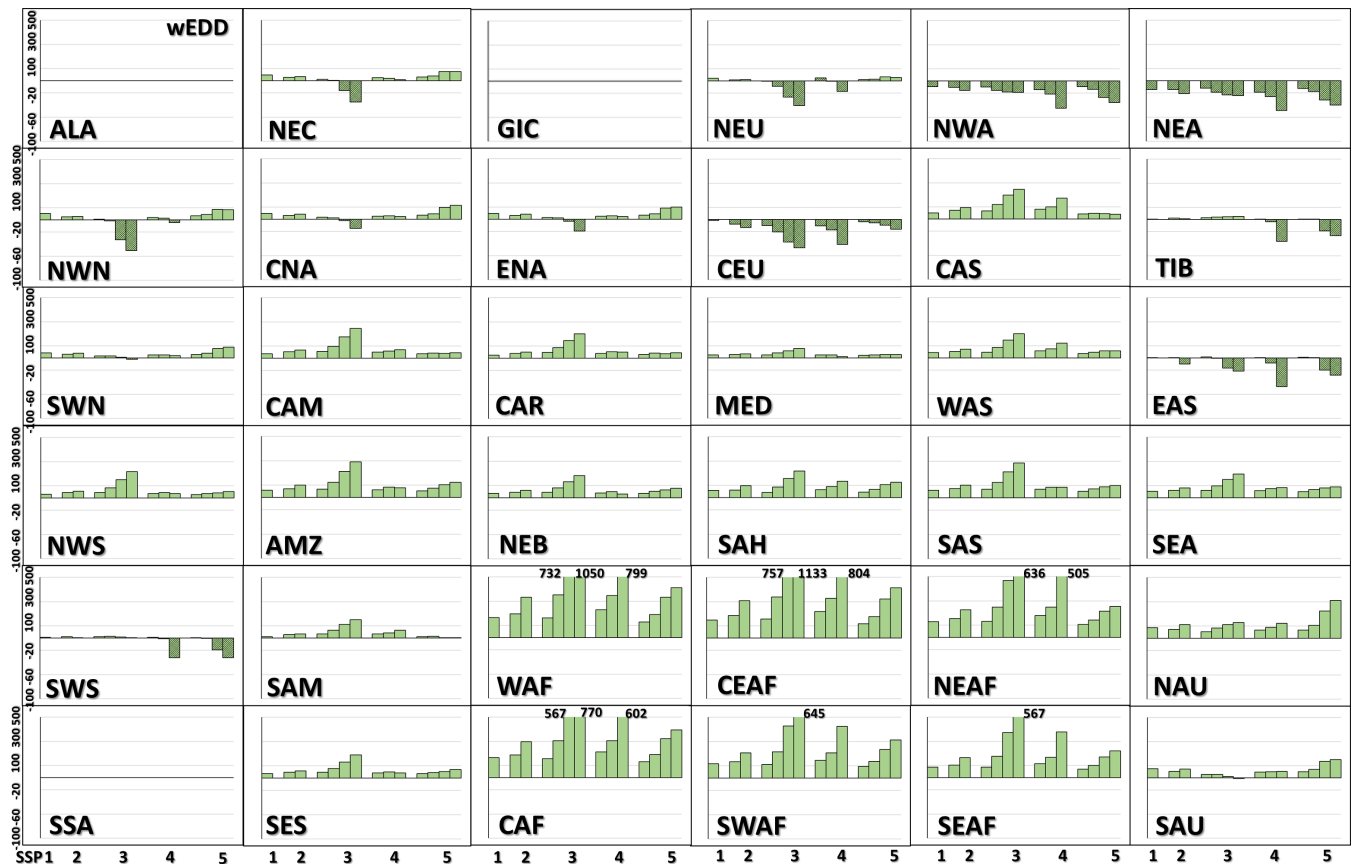


**FIGURE 7** Macro-regional energy degree-days projected change (%) from 1981–2010 to four GWLs and following five SSPs. Note: See Figure S2 for macro-regions. GWLs, global warming levels; SSPs, socio-economic scenarios; wEDD, weighted energy degree-days [Colour figure can be viewed at wileyonlinelibrary.com]

and decrease from GWL 2°C with other SSPs, resulting in small change with SSP2 (−5% at GWL 2°C) and more tangible decrease (between −30% and −36% at corresponding highest GWLs) with SSP3, SSP4, and SSP5. The combination of wCDD and wHDD results in the increase of wEDD with all SSPs: small with SSP1 (31% at GWL 1.5°C), medium with SSP2, SSP4, and SSP5 (44–49% at corresponding highest GWLs), and large with SSP3 (118%

at GWL 4°C). Despite the SSP4 does not allow reaching 4°C warming, wEDD are larger with SSP4 than SSP5, showing again the key role of population in degree-day projections. We highlight that the change in wCDD, wHDD, and wEDD should not be directly translated into change in energy but regarded as parameterization.

At macro-regional scale (Figure 7), we identify four groups regarding the projected change in wEDD: (A)

decrease irrespectively of the SSP; (B) increase irrespectively of the SSP; (C) increase or decrease depending on the SSP; (D) negligible change. Thus, climate plays the leading role in regions within Groups A and B and population does in regions within Group C.

Group A includes mid-latitude regions in Eurasia (central Europe, northwestern, northeastern, and eastern Asia) where, excluding SSP5 for central Europe and SSP3 for northwestern Asia, all SSPs project population decrease. However, the decrease in wHDD is likely to outbalance the decrease in wCDD with no exception, resulting in decreased total energy to cool and heat the environments with any RCP–SSP combination.

Group B includes 21 regions, mostly at tropical and equatorial latitudes: the entire Central and South America (excluding southern and southwestern South America), Africa, the Mediterranean region, and hot dry (western and central) and humid (southern and southeastern) Asia. In these regions, the combined increase in both wCDD and population is likely to result in increased energy to heat and cool the environments with any RCP–SSP combination.

Group C includes mid and high-latitude regions in North America (northwestern, southwestern, central, and eastern North America, and northeastern Canada) and (northern) Europe, where wEDD are projected to increase under all SSPs but SSP3 (decrease) and also SSP4 for northern Europe (decrease), that is, scenarios characterized by population decrease or not robust increase in such regions. Group C also includes two high-elevation and low populated regions (southwestern South America and Tibetan Plateau), where the decrease in wEDD is likely to increase with SSP1, SSP2, and SSP3 and decrease with SSP4 and SSP5.

Group D includes the high-latitude regions in both Hemispheres, where the extremely low or null population leads to negligible wEDD with any RCP–SSP combination.

## 5 | CONCLUSIONS

Starting from a large ensemble of CORDEX-based climate simulations based on two RCPs, we investigated projections of cooling, heating, and energy degree-days for GWLs from 1.5°C to 4°C. Subsequently, we applied population weighting (according to five SSPs to account for different roads of global development) in order to analyse the combined effects of climate and socio-economic scenarios on future energy demand to maintain thermal comfort in residential buildings.

The increase in CDD and decrease in HDD becomes larger with increasing GWL and most global lands show

statistically significant projections from 3°C warming. Therefore, EDD are projected to decrease at high latitudes and increase at equatorial and tropical latitudes, with approximately 50% of global lands with increasing EDD. Our results agree with those reported for North America by Petri and Caldeira (2015) and with general tendency in temperate climates (decrease in HDD larger than increase in CDD; Lemonsu *et al.*, 2013; You *et al.*, 2014; Zubler *et al.*, 2014) and tropical climates (increase in CDD larger than decrease in HDD; Mourshed, 2011; Mishra and Ramgopal, 2015; Khalyani *et al.*, 2016).

According to our analyses, with population weighting, though the SSP plays a crucial role, wEDD show the largest increase over equatorial Africa and India and the largest decrease over central Europe and China. Shi *et al.* (Shi *et al.*, 2016; Shi *et al.*, 2018) have reported similar results over China. Globally, wCDD are likely to increase with all SSPs (the largest with SSP3), while wHDD are likely to decrease with less sustainable SSPs (SSP3–SSP5) and show very small change with SSP1 and SSP2. Thus, wEDD are projected to overall increase at global scale, but to decrease over mid and high latitudes in Eurasia and in southwestern South America.

The presented population-weighted degree-day projections will be hosted by the European Commission's Data Risk Hub (<https://drmkc.jrc.ec.europa.eu/risk-data-hub>). Being aware of the assumptions and uncertainties discussed in previous sections, our results could be used by policy makers and stakeholders to implement strategies to optimize the energy used to keep thermal indoor comfort (Collins *et al.*, 2010; Ren *et al.*, 2010; Yang *et al.*, 2014) and possibly mitigate the increasing demand (Abrahamse and Shwom, 2018).

Starting from methodologies and results discussed in this paper, we will move in two directions. Firstly, we will focus at large metropolitan areas with specific local thresholds for CDD and HDD (Asdrubali *et al.*, 2008). Secondly, we will compute projections of growing degree-days (GDD; McMaster and Wilhelm, 1997), which could be used to, for example, predict plant stages (Miller *et al.*, 2001), estimate crop production (Parthasarathi *et al.*, 2013), and model growing season of various cultivars (Linderholm, 2006; Kukul and Irmak, 2018). To do that, we plan to use the newest version of climate simulations, the CMIP6 runs (Eyring *et al.*, 2016; Stouffer *et al.*, 2017).

## AUTHOR CONTRIBUTIONS

**Jonathan Spinoni:** Conceptualization; data curation; formal analysis; investigation; methodology; software; supervision; validation; visualization; writing - original draft; writing-review & editing. **Paulo Barbosa:**

Conceptualization; writing-review & editing. **Hans-Martin Fuessel**: Conceptualization; methodology; writing-review & editing. **Niall McCormick**: Writing-review & editing. **Juergen Vogt**: Writing-review & editing. **Alessandro Dosio**: Conceptualization; methodology; supervision; validation; visualization; writing - original draft; writing-review & editing.

## ORCID

Jonathan Spinoni  <https://orcid.org/0000-0002-8903-085X>

## REFERENCES

- Abrahamse, W. and Shwom, R. (2018) Domestic energy consumption and climate change mitigation. *Wiley Interdisciplinary Reviews: Climate Change*, 9(4), e525.
- Ahmed, T., Muttaqi, K.M. and Agalgaonkar, A.P. (2012) Climate change impacts on electricity demand in the State of New South Wales, Australia. *Applied Energy*, 98, 376–383.
- Allen, J.C. (1976) A modified sine wave method for calculating degree days. *Environmental Entomology*, 5(3), 388–396.
- Alola, A.A., Saint Akadiri, S., Akadiri, A.C., Alola, U.V. and Fatigun, A.S. (2019) Cooling and heating degree days in the US: the role of macroeconomic variables and its impact on environmental sustainability. *Science of the Total Environment*, 695, 133832.
- Asdrubali, F., Bonaut, M., Battisti, M. and Venegas, M. (2008) Comparative study of energy regulations for buildings in Italy and Spain. *Energy and Buildings*, 40(10), 1805–1815.
- Atalla, T., Gualdi, S. and Lanza, A. (2018) A global degree days database for energy-related applications. *Energy*, 143, 1048–1055.
- Auffhammer, M., Baylis, P. and Hausman, C.H. (2017) Climate change is projected to have severe impacts on the frequency and intensity of peak electricity demand across the United States. *Proceedings of the National Academy of Sciences*, 114(8), 1886–1891.
- Auffhammer, M. and Mansur, E.T. (2014) Measuring climatic impacts on energy consumption: a review of the empirical literature. *Energy Economics*, 46, 522–530.
- Azose, J.J., Ševčíková, H. and Raftery, A.E. (2016) Probabilistic population projections with migration uncertainty. *Proceedings of the National Academy of Sciences of the United States of America*, 113(23), 6460–6465.
- Batibeniz, F., Ashfaq, M., Diffenbaugh, N.S., Key, K., Evans, K.J., Turuncoglu, U.U. and Öno, B. (2020) Doubling of US population exposure to climate extremes by 2050. *Earth's Future*, 8(4), e2019EF001421.
- Bauer, N., Calvin, K., Emmerling, J., Fricko, O., Fujimori, S., Hilaire, J., Eom, J., Krey, V., Kriegler, V., Mouratiadou, I., de Boer, H.S., van den Berg, M., Carrara, S., Daioglu, V., Drouet, L., Edmonds, J.E., Gernaat, D., Havlik, P., Johnson, N., Klein, D., Kyle, P., Marangoni, G., Masui, T., Pietzcker, R. C., Strubegger, M., Wise, M., Riahi, K. and van Vuuren, D. (2017) Shared socio-economic pathways of the energy sector—quantifying the narratives. *Global Environmental Change*, 42, 316–330.
- Buceti, G. (2015) Climate change and vulnerabilities of the European energy balance. *Journal of Sustainable Development of Energy, Water and Environment Systems*, 3(1), 106–117. <https://doi.org/10.13044/j.sdewes.2015.03.0008>.
- Calvin, K., Bond-Lamberty, B., Clarke, L., Edmonds, J., Eom, J., Hartin, C., Kim, S., Kyle, P., Link, R., Moss, R., McJeon, H., Patel, P. and Stephanie, S.S. (2017) The SSP4: a world of deepening inequality. *Global Environmental Change*, 42, 284–296.
- Christenson, M., Manz, H. and Gyalistras, D. (2006) Climate warming impact on degree-days and building energy demand in Switzerland. *Energy Conversion and Management*, 47(6), 671–686.
- Collins, L., Natarajan, S. and Levermore, G. (2010) Climate change and future energy consumption in UK housing stock. *Building Services Engineering Research and Technology*, 31(1), 75–90.
- Damm, A., Köberl, J., Pretenthaler, F., Rogler, N. and Töglhofer, C. (2017) Impacts of +2 C global warming on electricity demand in Europe. *Climate Services*, 7, 12–30.
- Day, A.R. and Karayiannis, T.G. (1999) Identification of the uncertainties in degree-day-based energy estimates. *Building Services Engineering Research and Technology*, 20(4), 165–172.
- Day, A.R., Maidment, G.G. & Ratcliffe, M.S. (2000) Cooling degree-days and their applicability to building energy estimation. In *20: 20 Vision: CIBSE/ASHRAE Conference*.
- De Dear, R.J., Akimoto, T., Arens, E.A., Brager, G., Candido, C., Cheong, K.W.D., Li, B., Nishihara, N., Sekhar, S.C., Tanabe, S., Toftum, J., Zhang, H. and Zhu, Y. (2013) Progress in thermal comfort research over the last twenty years. *Indoor Air*, 23(6), 442–461.
- De Rosa, M., Bianco, V., Scarpa, F. and Tagliafico, L.A. (2015) Historical trends and current state of heating and cooling degree days in Italy. *Energy Conversion and Management*, 90, 323–335.
- Dirks, J.A., Gorrisen, W.J., Hathaway, J.H., Skorski, D.C., Scott, M. J., Pulsipher, T.C., Huang, M., Liu, Y. and Rice, J.S. (2015) Impacts of climate change on energy consumption and peak demand in buildings: a detailed regional approach. *Energy*, 79, 20–32.
- Dosio, A. (2016) Projections of climate change indices of temperature and precipitation from an ensemble of bias-adjusted high-resolution EURO-CORDEX regional climate models. *Journal of Geophysical Research: Atmospheres*, 121(10), 5488–5511.
- Dosio, A. and Fischer, E.M. (2018) Will half a degree make a difference? Robust projections of indices of mean and extreme climate in Europe under 1.5 C, 2 C, and 3 C global warming. *Geophysical Research Letters*, 45(2), 935–944.
- Dosio, A., Jones, R.G., Jack, C., Lennard, C., Nikulin, G. and Hewitson, B. (2019) What can we know about future precipitation in Africa? Robustness, significance and added value of projections from a large ensemble of regional climate models. *Climate Dynamics*, 53(9–10), 5833–5858.
- Dounis, A.I. and Caraiacos, C. (2009) Advanced control systems engineering for energy and comfort management in a building environment—a review. *Renewable and Sustainable Energy Reviews*, 13(6–7), 1246–1261.
- EEA. (2019). *Heating and cooling degree-days*. Available from: [https://www.eea.europa.eu/ds\\_resolveuid/IND-348-en](https://www.eea.europa.eu/ds_resolveuid/IND-348-en) [Accessed 15th January 2021].
- Eyring, V., Bony, S., Meehl, G.A., Senior, C.A., Stevens, B., Stouffer, R.J. and Taylor, K.E. (2016) Overview of the coupled model intercomparison project phase 6 (CMIP6) experimental design and organization. *Geoscientific Model Development*, 9(5), 1937–1958.

- Fantini, L. and Schenone, C. (2001) Degree-days, population distribution and heating energy consumption: the Italian case. *International Journal of Ambient Energy*, 22(4), 199–210.
- Field, C.B., Barros, V.R., Dokken, D.J., Mach, K.J., Mastrandrea, M. D., Bilir, T.E., Chatterjee, M., Ebi, K.L., Estrada, Y.O., Genova, R.C., Girma, B., Kissel, E.S., Levy, A.N., MacCracken, S., Mastrandrea, P.R. and White, L.L. (2014) Summary for policymakers. In: *Climate Change 2014: Impacts, Adaptation, and Vulnerability. Part A: Global and Sectoral Aspects. Contribution of Working Group II to the Fifth Assessment Report of the Intergovernmental Panel on Climate Change*. Cambridge, UK: Cambridge University Press, pp. 1–32.
- Fricko, O., Havlik, P., Rogelj, J., Klimont, Z., Gusti, M., Johnson, N., Kolp, P., Strubegger, M., Valin, H., Armann, M., Ermolieva, T., Forsell, N., Herrero, M., Heyes, C., Kindermann, G., Krey, V., McCollum, D.L., Obersteiner, M., Pachauri, S., Rao, S., Schmid, E., Schoepp, W. and Riahi, K. (2017) The marker quantification of the shared socioeconomic pathway 2: a middle-of-the-road scenario for the 21st century. *Global Environmental Change*, 42, 251–267.
- Fujimori, S., Hasegawa, T., Masui, T., Takahashi, K., Herran, D.S., Dai, H., Hijioka, Y. and Kainuma, M. (2017) SSP3: AIM implementation of shared socioeconomic pathways. *Global Environmental Change*, 42, 268–283.
- Gao, J. (2020) *Global 1-km Downscaled Population Base Year and Projection Grids Based on the Shared Socioeconomic Pathways, Revision 01*. Palisades, NY: NASA Socioeconomic Data and Applications Center (SEDAC).
- Gao, J. and O'Neill, B.C. (2020) Mapping global urban land for the 21st century with data-driven simulations and shared socioeconomic pathways. *Nature Communications*, 11(1), 1–12.
- Gattuso, J.-P., Magnan, A., Billé, R., Cheung, W.W.L., Howes, E.L., Joos, F., Allemand, D., Bopp, L., Cooley, S.R., Eakin, C.M., Hoegh-Guldberg, O., Kelly, R.P., Pörtner, H.-O., Rogers, A.D., Baxter, J.M., Laffoley, D., Osborn, D., Rankovic, A., Rochette, J., Sumaila, U.R., Treyer, S. and Turley, C. (2015) Contrasting futures for ocean and society from different anthropogenic CO<sub>2</sub> emissions scenarios. *Science*, 349(6243), aac4722.
- Guttman, N.B. (1983) Variability of population-weighted seasonal heating degree days. *Journal of Climate and Applied Meteorology*, 22(3), 495–501.
- Hansen, J., Ruedy, R., Sato, M. and Lo, K. (2010) Global surface temperature change. *Reviews of Geophysics*, 48(4), 1–29.
- Harris, I., Osborn, T.J., Jones, P. and Lister, D. (2020) Version 4 of the CRU TS monthly high-resolution gridded multivariate climate dataset. *Scientific Data*, 7(1), 1–18.
- Hausfather, Z. and Peters, G.P. (2020) Emissions—the ‘business as usual’ story is misleading. *Nature*, 577(7792), 618–620.
- Hawkins, E., Smith, R.S., Gregory, J.M. and Stainforth, D.A. (2016) Irreducible uncertainty in near-term climate projections. *Climate Dynamics*, 46(11–12), 3807–3819.
- Hawkins, E., Ortega, P., Suckling, E., Schurer, A., Hegerl, G., Jones, P., Joshi, M., Osborn, T.J., Masson-Delmotte, V., Mignot, J., Thorne, P. and van Oldenborgh, G.J. (2017) Estimating changes in global temperature since the preindustrial period. *Bulletin of the American Meteorological Society*, 98(9), 1841–1856.
- Holmes, C., Tett, S. and Butler, A. (2017) What is the uncertainty in degree-Day projections due to different calibration methodologies? *Journal of Climate*, 30(22), 9059–9075.
- Huang, J. and Gurney, K.R. (2016) The variation of climate change impact on building energy consumption to building type and spatiotemporal scale. *Energy*, 111, 137–153.
- Idchabani, R., Garoum, M. and Khaldoun, A. (2015) Analysis and mapping of the heating and cooling degree-days for Morocco at variable base temperatures. *International Journal of Ambient Energy*, 36(4), 190–198.
- IPCC. (2018) *Global Warming of 1.5°C. An IPCC Special Report on the Impacts of Global Warming of 1.5°C above Pre-Industrial Levels and Related Global Greenhouse Gas Emission Pathways, in the Context of Strengthening the Global Response to the Threat of Climate Change, Sustainable Development, and Efforts to Eradicate Poverty* [V. Masson-Delmotte, et al. (eds.)]. Geneva, Switzerland: World Meteorological Organization.
- Jiang, F., Li, X., Wei, B., Hu, R. and Li, Z. (2009) Observed trends of heating and cooling degree-days in Xinjiang Province, China. *Theoretical and Applied Climatology*, 97(3–4), 349–360.
- Jiang, L. and O'Neill, B.C. (2017) Global urbanization projections for the shared socioeconomic pathways. *Global Environmental Change*, 42, 193–199.
- Jones, B. and O'Neill, B.C. (2016) Spatially explicit global population scenarios consistent with the shared socioeconomic pathways. *Environmental Research Letters*, 11(8), 084003.
- Jones, B. and O'Neill, B.C. (2020) *Global One-Eighth Degree Population Base Year and Projection Grids Based on the Shared Socioeconomic Pathways, Revision 01*. Palisades, NY: NASA Socioeconomic Data and Applications Center (SEDAC).
- Jones, B., Tebaldi, C., O'Neill, B.C., Oleson, K. and Gao, J. (2018) Avoiding population exposure to heat-related extremes: demographic change vs climate change. *Climatic Change*, 146(3–4), 423–437.
- Kadioglu, M. and Şen, Z. (1999) Degree-day formulations and application in Turkey. *Journal of Applied Meteorology*, 38(6), 837–846.
- Kendon, M., McCarthy, M., Jevrejeva, S. and Legg, T. (2016). State of the UKClimate 2015, Met Office, Exeter, UK. Available at: <https://www.metoffice.gov.uk/>. [Accessed 14th January 2021].
- Khalyani, A.H., Gould, W.A., Harmsen, E., Terando, A., Quinones, M. and Collazo, J.A. (2016) Climate change implications for tropical islands: Interpolating and interpreting statistically downscaled GCM projections for management and planning. *Journal of Applied Meteorology and Climatology*, 55(2), 265–282.
- Kriegler, E., Bauer, N., Popp, A., Humpenöder, F., Leimbach, M., Strefler, J., Baumstark, L., Bodirsky, B.L., Hilaire, J., Klein, D., Mouratiadou, I., Weindl, I., Bertram, C., Dietrich, P., Luderner, G., Pehl, M., Pietzcker, R., Piontek, F., Lotze-Campen, H., Biewald, A., Bonsch, M., Giannousakis, A., Kreidenweis, U., Müller, C., Rolinski, S., Schultes, A., Schwanitz, J., Stevanovic, M., Calvin, K., Emmerling, J., Fujimori, S. and Edenhofer, O. (2017) Fossil-fueled development (SSP5): an energy and resource intensive scenario for the 21st century. *Global Environmental Change*, 42, 297–315.
- Kukul, M.S. and Irmak, S. (2018) US agro-climate in 20th century: growing degree days, first and last frost, growing season length, and impacts on crop yields. *Scientific Reports*, 8(1), 1–14.
- Le Tertre, A., Lefranc, A., Eilstein, D., Declercq, C., Medina, S., Blanchard, M., Chardon, Beno., Fabre, P.F., Jusot, J.-F., Pascal,



- L.P.C. and Ledrans, M. (2006) Impact of the 2003 heatwave on all-cause mortality in 9 French cities. *Epidemiology*, 17, 75–79.
- Lee, K., Baek, H.J. and Cho, C. (2014) The estimation of base temperature for heating and cooling degree-days for South Korea. *Journal of Applied Meteorology and Climatology*, 53(2), 300–309.
- Lemonsu, A., Kounkou-Arnaud, R., Desplat, J., Salagnac, J.L. and Masson, V. (2013) Evolution of the Parisian urban climate under a global changing climate. *Climatic Change*, 116(3–4), 679–692.
- Linderholm, H.W. (2006) Growing season changes in the last century. *Agricultural and Forest Meteorology*, 137(1–2), 1–14.
- Manzano-Agugliaro, F., Montoya, F.G., Sabio-Ortega, A. and García-Cruz, A. (2015) Review of bioclimatic architecture strategies for achieving thermal comfort. *Renewable and Sustainable Energy Reviews*, 49, 736–755.
- McMaster, G.S. and Wilhelm, W. (1997) Growing degree-days: one equation, two interpretations. *Agricultural and Forest Meteorology*, 87, 291–300.
- Miller, P., Lanier, W. and Brandt, S. (2001) Using growing degree days to predict plant stages. *Ag/Extension Communications Coordinator, Communications Services, Montana State University-Bozeman, Bozeman, MO*, 59717(406), 994–2721.
- Mishra, A.K. and Ramgopal, M. (2015) An adaptive thermal comfort model for the tropical climatic regions of India (Köppen climate type A). *Building and Environment*, 85, 134–143.
- Moore, J.L., Liang, S., Akullian, A. and Remais, J.V. (2012) Cautioning the use of degree-day models for climate change projections in the presence of parametric uncertainty. *Ecological Applications*, 22(8), 2237–2247.
- Mourshed, M. (2011) The impact of the projected changes in temperature on heating and cooling requirements in buildings in Dhaka, Bangladesh. *Applied Energy*, 88(11), 3737–3746.
- O'Neill, B.C., Kriegler, E., Ebi, K.L., Kemp-Benedict, E., Riahi, K., Rothman, D.S., van Ruijven, B.J., van Vuuren, D.P., Birkmann, J., Kok, K., Levy, M. and Solecki, W. (2017) The roads ahead: narratives for shared socioeconomic pathways describing world futures in the 21st century. *Global Environmental Change*, 42, 169–180.
- O'Neill, B.C., Kriegler, E., Riahi, K., Ebi, K.L., Hallegatte, S., Carter, T.R., Mathur, R. and van Vuuren, D.P. (2014) A new scenario framework for climate change research: the concept of shared socioeconomic pathways. *Climatic Change*, 122(3), 387–400.
- O'Neill, B.C., Tebaldi, C., van Vuuren, D.P., Eyring, V., Friedlingstein, P., Hurtt, G., Knutti, R., Kriegler, E., Lamarque, J.-F., Lowe, J., Meehl, G.A., Moss, R., Riahi, K. and Sanderson, B.M. (2016) The scenario model Intercomparison project (ScenarioMIP) for CMIP6. *Geoscientific Model Development*, 9, 3461–3482.
- Papakostas, K. and Kyriakis, N. (2005) Heating and cooling degree-hours for Athens and Thessaloniki, Greece. *Renewable Energy*, 30(12), 1873–1880.
- Parthasarathi, T., Velu, G. and Jeyakumar, P. (2013) Impact of crop heat units on growth and developmental physiology of future crop production: a review. *Journal of Crop Science and Technology*, 2(1), 2319–3395.
- Peeters, L., De Dear, R., Hensen, J. and D'haeseleer, W. (2009) Thermal comfort in residential buildings: comfort values and scales for building energy simulation. *Applied Energy*, 86(5), 772–780.
- Pérez-Lombard, L., Ortiz, J. and Pout, C. (2008) A review on buildings energy consumption information. *Energy and Buildings*, 40(3), 394–398.
- Petri, Y. and Caldeira, K. (2015) Impacts of global warming on residential heating and cooling degree-days in the United States. *Scientific Reports*, 5, 12427.
- Raftery, A.E., Alkema, L. and Gerland, P. (2014) Bayesian population projections for the United Nations. *Statistical Science: A Review Journal of the Institute of Mathematical Statistics*, 29(1), 58–68.
- Ren, J., Zhu, L., Wang, Y., Wang, C. and Xiong, W. (2010) Very low temperature radiant heating/cooling indoor end system for efficient use of renewable energies. *Solar Energy*, 84(6), 1072–1083.
- Riahi, K., Rao, S., Krey, V., Cho, C., Chirkov, V., Fischer, G., Kindermann, G., Nakicenovic, N. and Rafaj, P. (2011) RCP 8.5—a scenario of comparatively high greenhouse gas emissions. *Climatic Change*, 109(1–2), 33.
- Riahi, K., Van Vuuren, D.P., Kriegler, E., Edmonds, J., O'Neill, B.C., Fujimori, S., Bauer, N., Calvin, K., Dellink, R., Fricko, O., Lutz, W., Popp, A., Cuaresma, J.C., KC, S., Leimbach, M., Jiang, L., Kram, T., Rao, S., Emmerling, J., Ebi, K., Hasegawa, T., Havlik, P., Humpenoder, F., Da Silva, L.A., Smith, S., Stehfest, E., Bosetti, B., Eom, J., Germaat, D., Masui, T., Rogelj, J., Streffer, J., Drouet, L., Krey, V., Luderer, G., Harmsen, M., Takahashi, K., Baumstark, L., Doelman, J.C., Kainuma, M., Klimont, Z., Marangoni, G., Lotze-Campen, H., Obersteiner, M., Tabeau, A. and Tavoni, M. (2017) The shared socioeconomic pathways and their energy, land use, and greenhouse gas emissions implications: an overview. *Global Environmental Change*, 42, 153–168.
- Rogelj, J., Meinshausen, M. and Knutti, R. (2012) Global warming under old and new scenarios using IPCC climate sensitivity range estimates. *Nature Climate Change*, 2(4), 248–253.
- Sailor, D.J. and Pavlova, A.A. (2003) Air conditioning market saturation and long-term response of residential cooling energy demand to climate change. *Energy*, 28(9), 941–951.
- Samir, K.C. and Lutz, W. (2017) The human core of the shared socioeconomic pathways: population scenarios by age, sex and level of education for all countries to 2100. *Global Environmental Change*, 42, 181–192.
- Santamouris, M., Papanikolaou, N., Livada, I., Koronakis, I., Georgakis, C., Argiriou, A. and Assimakopoulos, D.N. (2001) On the impact of urban climate on the energy consumption of buildings. *Solar Energy*, 70(3), 201–216.
- Sathaye, J.A., Dale, L.L., Larsen, P.H., Fitts, G.A., Koy, K., Lewis, S. M. and de Lucena, A.F.P. (2013) Estimating impacts of warming temperatures on California's electricity system. *Global Environmental Change*, 23(2), 499–511.
- Shi, Y., Gao, X., Xu, Y., Giorgi, F. and Chen, D. (2016) Effects of climate change on heating and cooling degree days and potential energy demand in the household sector of China. *Climate Research*, 67(2), 135–149.
- Shi, Y., Zhang, D.F., Xu, Y. and Zhou, B.T. (2018) Changes of heating and cooling degree days over China in response to global warming of 1.5 C, 2 C, 3 C and 4 C. *Advances in Climate Change Research*, 9(3), 192–200.
- Sillmann, J., Kharin, V.V., Zwiers, F.W., Zhang, X. and Bronaugh, D. (2013) Climate extremes indices in the CMIP5 multimodel ensemble: part 2. Future climate projections. *Journal of Geophysical Research: Atmospheres*, 118(6), 2473–2493.

- Spinoni, J., Barbosa, P., Buchhignani, E., Cassano, J., Cavazos, T., Christensen, J.H., Christensen, O.B., Coppola, E., Evans, J., Geyer, B., Giorgi, F., Hadjinicolaou, P., Jacob, D., Katzfey, J., Koenigk, T., Laprise, R., Lennard, C.J., Kurnaz, L.M., Li, D., Llopart, M., McCormick, N., Naumann, G., Nikulin, G., Ozturk, T., Panitz, H.J., da Rocha, R.P., Rockel, B., Solman, S.A., Syktus, J., Tangang, F., Teichmann, C., Vautard, R., Vogt, J.V., Winger, K., Zittis, G. and Dosio, A. (2020) Future global meteorological drought hot spots: a study based on CORDEX data. *Journal of Climate*, 33(9), 3635–3661.
- Spinoni, J., Vogt, J. and Barbosa, P. (2015) European degree-day climatologies and trends for the period 1951–2011. *International Journal of Climatology*, 35(1), 25–36.
- Spinoni, J., Vogt, J.V., Barbosa, P., Dosio, A., McCormick, N., Bigano, A. and Füssel, H.M. (2018) Changes of heating and cooling degree-days in Europe from 1981 to 2100. *International Journal of Climatology*, 38, e191–e208.
- Stouffer, R.J., Eyring, V., Meehl, G.A., Bony, S., Senior, C., Stevens, B. and Taylor, K.E. (2017) CMIP5 scientific gaps and recommendations for CMIP6. *Bulletin of the American Meteorological Society*, 98(1), 95–105.
- Taleghani, M., Tenpierik, M., Kurvers, S. and Van Den Dobbelen, A. (2013) A review into thermal comfort in buildings. *Renewable and Sustainable Energy Reviews*, 26, 201–215.
- Taylor, B.L. (1981) Population-weighted heating degree-days for Canada. *Atmosphere-Ocean*, 19(3), 261–268.
- Taylor, K.E., Stouffer, R.J. and Meehl, G.A. (2012) An overview of CMIP5 and the experiment design. *Bulletin of the American Meteorological Society*, 93(4), 485–498.
- Thevenard, D. (2011) Methods for estimating heating and cooling degree-days to any base temperature. *ASHRAE Transactions*, 117(1), 884–892.
- Thomson, A.M., Calvin, K.V., Smith, S.J., Kyle, G.P., Volke, A., Patel, P., Delgado-Arias, S., Bond-Lamberty, B., Wise, M.A., Clarke, L.E. and Edmonds, J.A. (2011) RCP4.5: a pathway for stabilization of radiative forcing by 2100. *Climatic Change*, 109 (1–2), 77.
- Valor, E., Meneu, V. and Caselles, V. (2001) Daily air temperature and electricity load in Spain. *Journal of Applied Meteorology*, 40 (8), 1413–1421.
- Van Vuuren, D.P. and Carter, T.R. (2014) Climate and socio-economic scenarios for climate change research and assessment: reconciling the new with the old. *Climatic Change*, 122 (3), 415–429.
- Van Vuuren, D.P., Stehfest, E., Gernaat, D.E., Doelman, J.C., Van den Berg, M., Harmsen, M., de Boer, H.S., Bouwman, L.F., Daioglou, V., Edelenbosch, O.Y., Girod, B., Kram, T., Lassaletta, L., Lucas, P.L., van Meijl, H., Muller, C., van Ruijven, B.J., van der Sluis, S. and Tabebu, A. (2017). Energy, land-use and greenhouse gas emissions trajectories under a green growth paradigm. *Global Environmental Change*, 42, 237–250.
- Wagner, A., Gossauer, E., Moosmann, C., Gropp, T. and Leonhart, R. (2007) Thermal comfort and workplace occupant satisfaction—results of field studies in German low energy office buildings. *Energy and Buildings*, 39(7), 758–769.
- Yang, L., Yan, H. and Lam, J.C. (2014) Thermal comfort and building energy consumption implications—a review. *Applied Energy*, 115, 164–173.
- You, Q., Fraedrich, K., Sielmann, F., Min, J., Kang, S., Ji, Z., Zhu, X. and Ren, G. (2014) Present and projected degree days in China from observation, reanalysis and simulations. *Climate Dynamics*, 43(5–6), 1449–1462.
- Zhao, H.X. and Magoulès, F. (2012) A review on the prediction of building energy consumption. *Renewable and Sustainable Energy Reviews*, 16(6), 3586–3592.
- Zhou, Y., Eom, J. and Clarke, L. (2013) The effect of global climate change, population distribution, and climate mitigation on building energy use in the US and China. *Climatic Change*, 119 (3–4), 979–992.
- Zubler, E.M., Scherrer, S.C., Croci-Maspoli, M., Liniger, M.A. and Appenzeller, C. (2014) Key climate indices in Switzerland; expected changes in a future climate. *Climatic Change*, 123(2), 255–271.

## SUPPORTING INFORMATION

Additional supporting information may be found online in the Supporting Information section at the end of this article.

**How to cite this article:** Spinoni, J., Barbosa, P., Füssel, H.-M., McCormick, N., Vogt, J. V., & Dosio, A. (2021). Global population-weighted degree-day projections for a combination of climate and socio-economic scenarios. *International Journal of Climatology*, 41(11), 5447–5464. <https://doi.org/10.1002/joc.7328>